

FABRICATION OF HEXAGONAL ZINC OXIDE NANORODS ON SEEDED
SUBSTRATE VIA HYDROTHERMAL METHOD

NURUL AMIERA SHAHIDA BINTI MAAROF

A thesis submitted in
fulfillment of the requirement for the award of the
Degree of Master of Electrical Engineering



PTT UTHM
PERPUSTAKAAN TUN AMINAH

Faculty of Electrical and Electronic Engineering
Universiti Tun Hussein Onn Malaysia

SEPTEMBER 2022

To my beloved parents and family members,
thank you for the endless love, support and encouragement throughout this journey.

Maarof Abd Razak

Zainon Jayos

Nurul Sazlina Maarof

Mohd Fariz Maarof

Nurul Nadiah Maarof

Mohamad Aidil Amar Mazalan



PTT AUTHM
PERPUSTAKAAN TUNKU TUN AMINAH

ACKNOWLEDGEMENT

Firstly, I would like to express my humble thanks to ALLAH S.W.T for this beautiful yet exciting journey in completing this project.

Next, I wish to express my sincerest appreciation to my supervisor, Assoc. Prof. Ts. Dr. Mohd Khairul bin Ahmad for his continuous support, encouragement and patience throughout the entire process.

Special thanks to Microelectronics & Nanotechnology – Shamsuddin Research Centre (MiNT-SRC), Universiti Tun Hussein Onn Malaysia (UTHM) for allowing me to use X-ray diffraction (XRD), field-emission scanning electron microscopy (FESEM), atomic force microscopy (AFM), ultraviolet-visible (UV-Vis) and four-point probe measurement.

I would like to acknowledge all MiNT-SRC technicians, Mrs. Faezahana, Mr Ahmad Nasrull, Mr Mohd Azwadi, my fellow friends (Anis Zafirah Mohd Ismail, Lai Chee Fung, Siti Nurhaziqah Abd Majid, Shazleen Ahmad Ramli and Diani Galih Saputri), and all post-graduate students that help me to finish up this thesis.

Lastly, I also like to express my special thanks to everyone who are involved directly or indirectly in this journey.

ABSTRACT

Zinc oxide (ZnO) has been studied due to have a direct wide bandgap (~3.7 eV), large exciton binding energy (~60 meV), non-toxic material. In this study, two step hydrothermal process was introduced to fabricate seed layer in a form of ZnO nanoparticles (ZnO-NPs) and ZnO nanorods (ZnO-NRs). The seed layer solution concentration is 0.3 M and consists of zinc acetate dihydrate (ZAD) and diethanolamine (DEA). Besides that, 5 layers of coated seed layer was deposited using spin coating method. Subsequently, the high quality of aligned hexagonal ZnO-NRs were fabricated using hydrothermal method which consists of an equimolar nutrient solution (0.05 M) synthesized using zinc nitrate hexahydrate (ZNH) and hexamethylenetetramine (HMTA). The hydrothermal reaction times were varied from 1 hour to 9 hours. The structural, morphological, topological, optical and electrical properties of the ZnO-NRs were studied using X-ray diffraction (XRD), Field-Emission Scanning Electron Microscopy (FESEM), Atomic Force Microscopy (AFM), Ultraviolet-visible (UV-Vis) spectroscopy and four-point probe, respectively. Based on the research, the deposition of ZnO-NPs indicated a significant improvement in the well-developed and aligned hexagonal of ZnO-NRs. As a result, ZnO-NRs synthesized with 6 hours of hydrothermal reaction time had an average diameter of 185 nm and rod lengths of 2.04 μ m. However, recorded the lowest value of resistivity ($0.83 \times 10^{-3} \Omega \cdot \text{cm}$) thus, exhibited the highest value of conductivity ($12.11 \times 10^2 \Omega \cdot \text{cm}^{-1}$). As higher conductivity materials can transfer more electrons, thereby increasing the rate of electron-hole generation. This will lead to greater current flows. Therefore, ZnO-NRs can be widely implemented in electronic devices application such as ultraviolet sensor and thermoelectric application.

ABSTRAK

Zink oksida (ZnO) telah dikaji kerana mempunyai jalur lebar langsung ($\sim 3.7 \text{ eV}$), tenaga pengikatan *exciton* yang besar ($\sim 60 \text{ meV}$) dan bahan tidak bertoksik. Dalam kajian ini, proses hidroterma dua langkah diperkenalkan untuk membuat lapisan biji benih dalam bentuk ZnO nanopartikel (ZnO-NPs) dan ZnO nanorod (ZnO-NRs). Kepekatan larutan lapisan biji benih adalah 0.3 M dan terdiri daripada zink asetat dihidrat (ZAD) dan dietanolamina (DEA). Selain daripada itu, 5 lapisan biji benih yang disalut didepositkan menggunakan kaedah salutan pusingan. Seterusnya, ZnO-NRs yang berkualiti tinggi dan mempunyai bentuk heksagonal yang sejajar dibuat menggunakan kaedah hidroterma yang terdiri daripada larutan nutrien setara (0.05 M) yang disintesis menggunakan zink nitrat heksahidrat (ZNH) dan heksametilenetramina (HMTA). Masa tindak balas hidroterma adalah berbeza-beza dari 1 jam hingga 9 jam. Sifat struktur, morfologi, topologi, optik dan elektrik bagi ZnO-NRs dikaji menggunakan difraksi sinar-X (XRD), Mikroskopi Elektronik Pengimbasan Pancaran Medan (FESEM), Mikroskopi Daya Atom (AFM), spektroskopi tampak *Ultraviolet* (UV-Vis) dan kuar empat titik. Berdasarkan penyelidikan, pemendapan ZnO-NPs menunjukkan peningkatan yang ketara dalam ZnO-NRs yang berbentuk heksagon yang dibangunkan dengan baik dan sejajar. Hasilnya, ZnO-NRs yang disintesis dengan 6 jam masa tindak balas hidroterma mempunyai diameter purata 185 nm dan panjang nanorod $2.04 \mu\text{m}$. Walau bagaimanapun, mencatatkan nilai resistiviti yang paling rendah ($0.83 \times 10^{-3} \Omega.\text{cm}$) dan dengan itu, menunjukkan nilai kekonduksian yang paling tinggi ($12.11 \times 10^2 \Omega.\text{cm}^{-1}$). Oleh kerana bahan kekonduksian yang lebih tinggi boleh memindahkan lebih banyak elektron, dengan itu meningkatkan kadar penjanaan *electron-hole*. Ini akan membawa kepada aliran arus elektrik yang lebih besar. Oleh itu, ZnO-NRs boleh dilaksanakan secara meluas dalam peranti aplikasi elektronik seperti penderia ultraungu dan aplikasi termoelektrik.

CONTENTS

TITLE	i
DECLARATION	ii
DEDICATION	iii
ACKNOWLEDGEMENT	iv
ABSTRACT	v
ABSTRAK	vi
CONTENTS	vii
LIST OF TABLES	xii
LIST OF FIGURES	xii
LIST OF SYMBOLS AND ABBREVIATIONS	xviii
LIST OF PUBLICATIONS	xxi
LIST OF AWARD	xxii
CHAPTER 1 INTRODUCTION	1
1.1 Research background	1
1.2 Problem statement	3
1.3 Objectives of the study	4
1.4 Scopes of the study	4
1.5 Research contribution	4
1.6 Outline of the thesis	5
CHAPTER 2 LITERATURE REVIEW	7
2.1 Introduction	7

2.2 Zinc oxide nanostructures	7
2.2.1 Zinc oxide nanoparticles as seed layer	8
2.2.1.1 Fabrication methods for ZnO-NPs	9
2.2.1.2 Growth mechanism of ZnO-NPs as seed layer using spin coating method	12
2.2.2 Zinc oxide nanorods	12
2.2.2.1 Fabrication methods for ZnO-NRs	13
2.2.2.2 Growth mechanism of hexagonal ZnO-NRs via hydrothermal method	18
2.3 Summary	22
CHAPTER 3 METHODOLOGY	23
3.1 Introduction	23
3.2 FTO substrate cleaning process	24
3.3 Deposition of ZnO-NPs as a seed layer using spin coating method	25
3.3.1 Seed layer solution preparation	26
3.3.2 Seed layer deposition process	26
3.4 Fabrication of ZnO-NRs on seeded FTO substrate via hydrothermal process	29
3.4.1 Hydrothermal nutrient solution preparation	29
3.4.2 Hydrothermal process	30
3.5 Characterization method of ZnO-NPs and ZnO-NRs	31
3.5.1 Structural properties	32
3.5.2 Morphological properties	34
3.5.3 Topological properties	37
3.5.4 Optical properties	39

3.5.5 Electrical properties	41
3.6 Summary	42
CHAPTER 4 RESULT AND DISCUSSIONS	44
4.1 Introduction	44
4.2 The influence of seed layer solution concentration towards the ZnO-NPs and ZnO-NRs	45
4.2.1 Structural properties	45
4.2.2 Morphological properties	48
4.2.3 Topological properties	55
4.2.4 Optical properties	57
4.2.5 Electrical properties	58
4.2.6 Summary on the influence of seed layer solution concentration towards the ZnO-NPs and ZnO-NRs	59
4.3 The effect of using different numbers of coated seed layers on ZnO-NPs and ZnO-NRs	60
4.3.1 Structural properties	60
4.3.2 Morphological properties	62
4.3.3 Topological properties	68
4.3.4 Optical properties	69
4.3.5 Electrical properties	70
4.3.6 Summary on the effect of using different numbers of coated seed layers on ZnO-NPs and ZnO-NRs	71
4.4 The impact of using various hydrothermal reaction times on ZnO-NRs	71
4.4.1 Structural properties	72
4.4.2 Morphological properties	73
4.4.3 Optical properties	77

4.4.4 Electrical properties	78
4.4.6 Summary on the impact of using various hydrothermal reaction times on ZnO nanorods	79
CHAPTER 5 CONCLUSION AND RECOMMENDATION	80
5.1 Introduction	80
5.2 Conclusion	80
5.3 Recommendation	82
REFERENCES	83



PTTA UTHM
PERPUSTAKAAN TUNKU TUN AMINAH

LIST OF TABLES

2.1	Comparison of the method used to fabricate ZnO nanostructures.	17
2.2	Comparison of the method used to fabricate ZnO nanostructures (continued).	18
2.3	Comparison of ZnO-NRs growth assisted by alkaline or HMTA aqueous solutions.	21
3.1	Variation of experimental parameters.	24
3.2	The details of seed layer deposition process.	27
3.3	The details of seed layer deposition process (continued).	28
4.1	The summary of parameters for the first optimization process.	45
4.2	The data of ZnO-NRs fabricated with different seed layer solution concentration at (002) plane obtained from XRD analysis.	48
4.3	The average diameter and length of ZnO thin film fabricated using different seed layer solution concentration.	55
4.4	The summary of parameters for the second optimization process.	60
4.5	The data of ZnO-NRs fabricated with different numbers of coated seed layers at (002) plane obtained from XRD analysis.	62
4.6	The average diameter and length of ZnO thin film fabricated using different number of coated seed layer.	66
4.7	The summary of parameters for the third optimization process.	72
4.8	The data of ZnO-NRs fabricated with various of hydrothermal reaction time at (002) plane obtained from XRD analysis.	73
4.9	The average diameter and length of ZnO thin film prepared at various of hydrothermal reaction time.	77

LIST OF FIGURES

1.1	The crystal structure of ZnO: (a) Cubic rocksalt, (b) Cubic zinc blende and (c) Hexagonal wurtzite atom.	2
1.2	Schematic representation of ZnO wurtzite structure.	3
2.1	The morphology of ZnO; (a) nanoflowers, nanoparticles, (c) nanoplates and (d) nanorods.	8
2.3	The illustration of drop-casting method.	10
2.4	The illustration of dip coating process that consists of three steps; (i) dipping, (ii) deposition and drainage and (iii) evaporation.	10
2.5	The illustration of spin coating process that consists of four steps; (i) deposition, (ii) spin up, (iii) spin off and (iv) evaporation.	11
2.6	The schematic of MBE growth system to fabricate ZnO.	14
2.7	The schematic diagram of PLD experiment set-up.	14
2.8	The schematic diagram of electrochemical deposition process for deposition of ZnO.	15
2.9	The schematic diagram of CBD process.	15
2.10	The images of: (a) hexagonal ZnO crystal with no attachment ions and (b) possible attachment of OH ⁻ ions on the non-polar facets.	21
3.1	The illustration of (a) FTO substrate, (b) ZnO-NPs after spin coated process and (c) ZnO-NRs after hydrothermal process.	23
3.2	The images of FTO substrate: (a) substrate dimension and (b) illustration of cross-section.	24
3.3	FTO substrate cleaning process flow.	25

3.4	The illustration of FTO substrate cross-section images: (a) before and (b) after seed layer deposition process.	25
3.5	The seed layer solution materials: (a) zinc acetate dihydrate (ZAD), (b) diethanolamine (DEA) and (c) ethanol.	26
3.6	The illustration of FTO substrate cross-section images: (a) before and (b) after hydrothermal process.	29
3.7	The images of materials used for hydrothermal nutrient solution: (a) zinc nitrate hexahydrate (ZNH) and (b) hexamethylenetetramine (HMTA).	30
3.8	The illustration image of the blue cap reagent bottle with the position of seeded FTO substrate during hydrothermal process.	31
3.9	The hydrothermal process flow.	31
3.10	XRD machine (PANalytical X-Pert3 Powder) used to characterize the structural properties of the samples.	32
3.11	(a) Diffraction from two scattering planes, (b) X-ray Diffractogram.	33
3.12	The examples of XRD patterns of ZnO-NRs on FTO substrate by using hydrothermal process.	34
3.13	The FESEM instrument (JEOL-JSM 7600F) was used to characterize the morphological properties of the samples.	35
3.14	Schematic working principle of typical SEM and FESEM.	36
3.15	The example results of FESEM images of ZnO-NRs by using hydrothermal process on FTO substrate.	37
3.16	The AFM instrument used to characterize topological properties of the samples.	38
3.17	The schematic of AFM working principle.	38
3.18	The example results of topological properties measurement of ZnO nanostructures regarding to ZnO seed layer (a and b) annealed at low temperature and (c and d) annealed at high temperature.	39
3.19	The UV-Vis spectroscopy (Shimadzu UV-1800 240V) used to characterize the optical properties of the samples.	40

3.20	The example results of optical properties measurement of ZnO nanostructures regarding to (a) the transmittance and (b) the Tauc's plot.	41
3.21	The schematic diagram of a four-point probe circuit.	42
3.22	Four-point probes system (Pro4-4000 Four Point Resistivity Configurations) used to characterize the electrical properties of the samples.	42
4.1	FESEM result of FTO (a) surface morphology and (b) illustration of cross-section image.	44
4.2	The XRD pattern of ZnO-NPs for different seed layer solution concentrations of (a) 0.1 M, (b) 0.3 M, (c) 0.5 M and (d) 0.7 M.	46
4.3	The XRD pattern of ZnO-NRs for different seed layer solution concentration of (a) 0.1 M, (b) 0.3 M, (c) 0.5 M and (d) 0.7 M.	47
4.4	The cross-section images of ZnO-NPs after spin coating process.	48
4.5	The FESEM images of top view ZnO-NPs at: (a) low magnification and (b) high magnification, fabricated using 0.1 M of seed layer solution concentrations.	49
4.6	The FESEM images of top view ZnO-NPs at: (a) low magnification and (b) high magnification, fabricated using 0.3 M of seed layer solution concentrations.	49
4.7	The FESEM images of top view ZnO-NPs at: (a) low magnification and (b) high magnification, fabricated using 0.5 M of seed layer solution concentrations.	50
4.8	The FESEM images of top view ZnO-NPs at: (a) low magnification and (b) high magnification, fabricated using 0.7 M of seed layer solution concentrations.	50
4.9	The illustrated cross section images of ZnO-NRs fabricated by using thin seed layer [23].	51
4.10	The illustration of ZnO-NRs cross-section images after hydrothermal process.	51

4.11	The FESEM images of top view ZnO-NRs at: (a) low magnification and (b) high magnification, fabricated using 0.1 M of seed layer solution concentrations.	52
4.12	The FESEM images of top view ZnO-NRs at: (a) low magnification and (b) high magnification, fabricated using 0.3 M of seed layer solution concentrations.	52
4.13	The FESEM images of top view ZnO-NRs at: (a) low magnification and (b) high magnification, fabricated using 0.5 M of seed layer solution concentrations.	53
4.14	The FESEM images of top view ZnO-NRs at: (a) low magnification and (b) high magnification, fabricated using 0.7 M of seed layer solution concentrations.	53
4.15	FESEM cross-sectional images of the ZnO-NRs thin film fabricated with different seed layer solution concentration; (a) 0.1 M, (b) 0.3 M, (c) 0.5 M and (d) 0.7 M.	54
4.16	The 3-D AFM micrograph of ZnO-NPs fabricated using different seed layer solution concentrations of (a) 0.1, (b), 0.3 M, (c) 0.5 M and (d) 0.7 M.	56
4.17	The graph of average surface roughness against seed layer concentration.	56
4.18	The optical band gap (E_g) from Tauc's plot of ZnO-NRs fabricated using different seed layer solution concentration (a) 0.1 M, (b) 0.3 M, (c) 0.5 M and (d) 0.7M.	57
4.19	The graph of different seed layer solution concentrations (0.1 M, 0.3 M, 0.5 M and 0.7 M) against resistivity and conductivity of ZnO-NRs.	59
4.20	The XRD pattern of ZnO-NPs fabricated using different numbers of coated seed layers (a) 1 L, (b) 3 L, (c) 5 L and (d) 8 L.	61
4.21	The XRD pattern of ZnO-NRs fabricated using different numbers of coated seed layers (a) 1 L, (b) 3 L, (c) 5 L and (d) 8 L.	61

4.22	The FESEM images of top view ZnO-NPs at: (a) low magnification and (b) high magnification, fabricated using 1 L of coated seed layer.	63
4.23	The FESEM images of top view ZnO-NPs at: (a) low magnification and (b) high magnification, fabricated using 3 L of coated seed layers.	63
4.24	The FESEM images of top view ZnO-NPs at: (a) low magnification and (b) high magnification, fabricated using 5 L of coated seed layers.	63
4.25	The FESEM images of top view ZnO-NPs at: (a) low magnification and (b) high magnification, fabricated using 8 L of coated seed layers.	64
4.26	The FESEM images of top view ZnO-NRs at: (a) low magnification and (b) high magnification, fabricated using 1 L of coated seed layer.	65
4.27	The FESEM images of top view ZnO-NRs at: (a) low magnification and (b) high magnification, fabricated using 3 L of coated seed layers.	65
4.28	The FESEM images of top view ZnO-NRs at: (a) low magnification and (b) high magnification, fabricated using 5 L of coated seed layers.	65
4.29	The FESEM images of top view ZnO-NRs at: (a) low magnification and (b) high magnification, fabricated using 8 L of coated seed layers.	66
4.30	FESEM cross-sectional images of i) ZnO-NPs and ii) ZnO-NRs fabricated using different number of coated seed layer (a) 1 L, (b) 3 L, (c) 5 L and (d) 8 L.	67
4.31	The 3-D AFM micrograph of ZnO-NPs fabricated using different number of coated seed layer (a) 1 L, (b) 3 L, (c) 5 L and (d) 8 L.	68
4.32	The graph of average surface roughness against number of coated seed layers.	69

4.33	The band gap estimation from Tauc's plot of ZnO-NRs fabricated using different number of coated seed layer (a) 1 L, (b) 3 L, (c) 5 L and (d) 8 L.	69
4.34	The graph of numbers of coated layers (1 L, 3 L, 5 L and 8 L) against resistivity and conductivity of ZnO-NRs.	70
4.35	The XRD pattern of ZnO-NRs prepared at various of hydrothermal reaction time (a) 1 h, (b) 3 h, (c) 6 h and (d) 9 h.	72
4.36	The illustration of cross-section images: (a) 5 coated seed layers after spin coating process and (b) ZnO-NRs after hydrothermal process.	73
4.37	The FESEM images of top view ZnO-NRs at: (a) low magnification and (b) high magnification, prepared at 1 h of hydrothermal reaction time.	74
4.38	The FESEM images of top view ZnO-NRs at: (a) low magnification and (b) high magnification, prepared at 3 h of hydrothermal reaction times.	75
4.39	The FESEM images of top view ZnO-NRs at: (a) low magnification and (b) high magnification, prepared at 6 h of hydrothermal reaction times.	75
4.40	The FESEM images of top view ZnO-NRs at: (a) low magnification and (b) high magnification, prepared at 9 h of hydrothermal reaction times.	76
4.41	FESEM cross-sectional images of ZnO-NRs prepared at various of hydrothermal reaction time (a) 1 h, (b) 3 h, (c) 6 h and (d) 9 h.	77
4.42	The band gap estimation from Tauc's plot of ZnO-NRs prepared at various of hydrothermal reaction time (a) 1 h, (b) 3 h, (c) 6 h and (d) 9 h.	78
4.43	The graph of ZnO-NRs prepared at various of hydrothermal reaction time (1 h, 3 h, 6 h and 9 h) against resistivity and conductivity.	79

LIST OF SYMBOLS AND ABBREVIATIONS

C	- Molar Concentration
D	- Average Crystallite Size
K	- Scherrer Constant, $K=0.94\text{\AA}$.
α	- Absorption Coefficient
δ	- Dislocation Density
E_g	- Bandgap Energy
E_w	- Lower Work Function
$h\nu$	- Photon Energy
$k_B T$	- Room Temperature Thermal Energy
R_a	- Average Surface Roughness
t	- Thickness of The Material
v	- Volume
λ	- Wavelength
ρ	- Resistivity
σ	- Conductivity
θ	- Incident Angle
ΔV	- Change In Voltage
1D	- One-Dimensional
2D	- Two-Dimensional
3D	- Three-Dimensional
AAO	- Anodic Aluminium Oxide
AFM	- Atomic Force Microscopy
CBD	- Chemical Bath Deposition
CdTe	- Cadmium Telluride

DEA	-	Diethanolamine
DI	-	Deionized Water
DSSC	-	Dye-Sensitized Solar Cells
ED	-	Electrochemical Deposition
FESEM	-	Field-Emission Scanning Electron Microscopy
FTO	-	Fluorine Doped Tin Oxide
FWHM	-	Full Width At Half Maximum
HMTA	-	Hexamethylenetetramine
HMTA	-	Hexamethylenetetramine
In ₂ O ₃	-	Indium Trioxide
ITO	-	Indium Tin Oxide
KCl	-	Potassium Chloride
KOH	-	Potassium Hydroxide
L	-	Number Of Coated Seed Layer
MBE	-	Molecular Beam Epitaxy
MgO	-	Magnesium Oxide
MW	-	Molecular Weight
NaCl	-	Sodium Chloride
NaOH	-	Sodium Hydroxide
O	-	Oxygen
PA-MBE	-	Plasma-Assisted Molecular Beam Epitaxy
PEI	-	Polyethylenimine
PLD	-	Pulsed Laser Deposition
SEM	-	Scanning Electron Microscope
SnO ₂	-	Tin Dioxide
TiO ₂	-	Titanium Dioxide
UV	-	Ultraviolet
UV-Vis	-	Ultraviolet-Visible
VDP	-	Van Der Pauw
WO ₃	-	Tungsten Trioxide
XRD	-	X-Ray Diffraction
ZAD	-	Zinc Acetate Dihydrate

Zn	-	Zinc
ZNH	-	Zinc Nitrate Hexahydrate
ZnO	-	Zinc Oxide
ZnO-NPs	-	Zinc Oxide Nanoparticles
ZnO-NRs	-	Zinc Oxide Nanorods
ZnS	-	Zinc Sulphide
ZnSO ₄	-	Zinc Sulfate
VDP	-	Van Der Pauw
WO ₃	-	Tungsten Trioxide
XRD	-	X-Ray Diffraction
ZAD	-	Zinc Acetate Dihydrate
ZNH	-	Zinc Nitrate Hexahydrate
ZnO	-	Zinc Oxide
ZnO-NPs	-	ZnO Nanoparticles
ZnO-NRs	-	ZnO Nanorods
ZnS	-	Zinc Sulphide

LIST OF PUBLICATIONS

Journal /Proceedings:

1. Shazleen Ahmad Ramli, Fariza Mohamad, A.G.A Anizam, M.K. Ahmad, Norazlina Ahmad, Anis Zafirah Mohd Ismail, Nurliyana Mohamad Arifin, **Nurul Amiera Shahida Maarof**, A.M.S Nurhaziqah, D.G Saputri, Nik Hisyamudin Muhd Nor and Izaki Masanobu, “Properties enhancement of TiO₂ nanorod thin film using hydrochloric acid etching treatment method”, *J Mater Sci: Mater Electron* 33, 16348–16356 (2022).
2. Nyaanalechumi Vijayan, **Nurul Amiera Shahida Maarof**, Nurul Huda Abdul Rahman, Mohd Khairul Ahmad, “Study of Zinc Oxide Nanoflower for Photocatalytic Applications Prepared via Hydrothermal Method”, *Evolution in Electrical and Electronic Engineering* Vol. 2No. 2, p. 10-17 (2021).
3. **Nurul Amiera Shahida Maarof**, Mohd Khairul Ahmad, Soon Chin Phong, Syafa Syahirah Taib, Nurhayati Muhd Ramli, Nafarizal Nayan, Mohamad Hafiz Mamat, Suriani Abu Bakar, Azmi Mohamed, Masaru Shimomura, “Fabrication and Characterization of Titanium Dioxide (TiO₂) Nanorods and Nanoflowers on Fluorine Doped Tin Oxide (FTO) for Ethanol Gas Sensor Application”, *International Journal of Emerging Trends in Engineering Research*, 8(1.2), 7 – 13 (2020).

LIST OF AWARD

Third place in FKEE Postgraduate Poster Day Conference, November 2019,
Universiti Tun Hussein Onn Malaysia.



CHAPTER 1

INTRODUCTION

1.1 Research background

Zinc oxide (ZnO) is one of the metal oxide semiconductor materials that has been extensively studied due to its unique properties. Other metal oxide semiconductor materials are indium trioxide (In_2O_3), tin dioxide (SnO_2), titanium dioxide (TiO_2), tungsten trioxide (WO_3) and zinc oxide (ZnO), which has special catalytic, anti-bacterial, as well as good optical and electrical properties [1],[2]. ZnO also known as an Earth abundant material which is non-toxic, chemically and thermally stable semiconductor material that has wide direct band gap energy (~3.37 eV). Thus, make it more preferable over the other wide-band-gap materials due to its high energy radiation stability and amenability to wet chemical etching [3]. This makes ZnO as a suitable candidate for space applications.

Meanwhile, large excitation binding energy of ~60 meV paves the way for an intense near-band-edge excitonic emission at room and high temperature [4], [5], [6]. ZnO has been considered as the most promising nanostructures material that has a wide range of application such as solar cells [7], photocatalyst [8], UV photodetector [9] and thermoelectric devices such as energy generators or cooling devices [10]. Moreover, ZnO exists in three crystal structures which are cubic rocksalt, cubic zinc blende, and hexagonal wurtzite, as shown in Figure 1.1 (a), 1.1 (b), and 1.1 (c), respectively were shaded with light green refers to zinc atom while shaded in dark green represents oxygen atom [11]. From these three structures, the wurtzite structure is the most stable structure under normal conditions while rocksalt structures can only fabricated at high pressure and zinc blende structures can only synthesized on cubic

substrates such as zinc sulphide (ZnS), cadmium telluride (CdTe), magnesium oxide (MgO), potassium chloride (KCl) and sodium chloride (NaCl) [3], [12]. The wurtzite structure is a hexagonal crystal system that belongs to the space group of $P6_3mc$ (No. 186), possesses two lattice parameters which are; $a=3.2495\text{\AA}$ and $c=5.2069\text{\AA}$ with a ratio of $c/a=1.63$ [3].

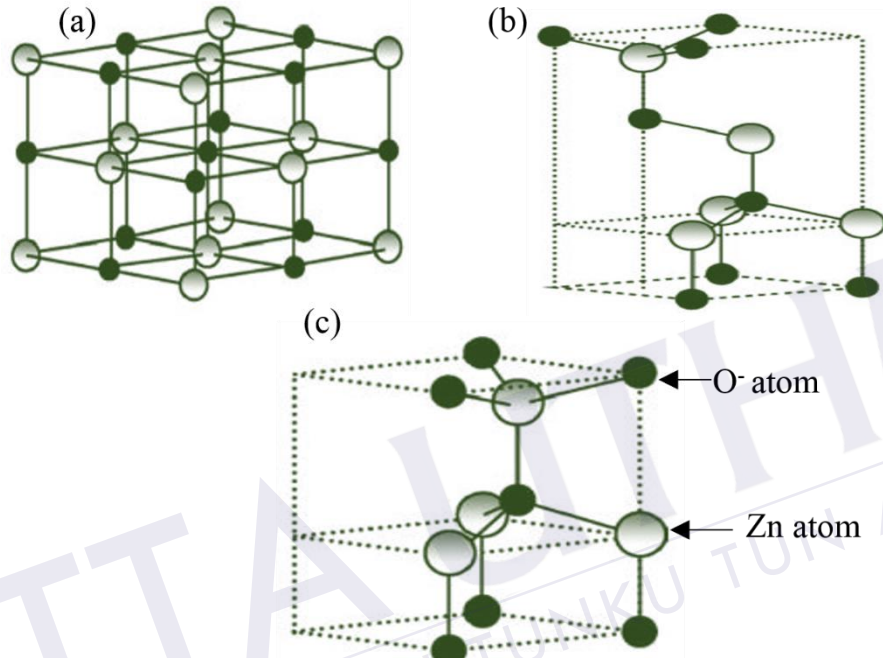


Figure 1.1:

Figure 1.1: The crystal structure of ZnO: (a) Cubic rocksalt, (b) Cubic zinc blende and (c) Hexagonal wurtzite atom [3].

A schematic representation of the wurtzite ZnO structure is shown in Figure 1.2. This shows that wurtzite crystal structure correlates with the ratio of an ideal crystal. Despite the fact that the ionic nature of Zn-O is quite strong, ZnO displays a little covalent bonding. These can be compared to the basal plane, which it has facets that exhibit massive surface reconstruction. In this structure, ZnO has high electron mobility and thermal conductivity in this form because of the sp^3 hybrid valence electrons in its wurtzite lattice structure [13]. Besides that, single crystal ZnO has high electrons mobility ($200-300 \text{ cm}^2\text{V}^{-1}\text{s}^{-1}$) at room temperature, which the great advantage in its electrical characteristics [13]. However, ZnO has high thermal conductivity and it is the main disadvantage for thermoelectric applications. The thermal conductivity

of pure ZnO at 300 K is around $49 \text{ Wm}^{-1}\text{K}^{-1}$ and drops to $10 \text{ Wm}^{-1}\text{K}^{-1}$ at 1000 K [17]. As a result, in addition to enhance the electrical conductivity, most attempts to improve the thermoelectric performance of pure ZnO focus on lowering thermal conductivity.

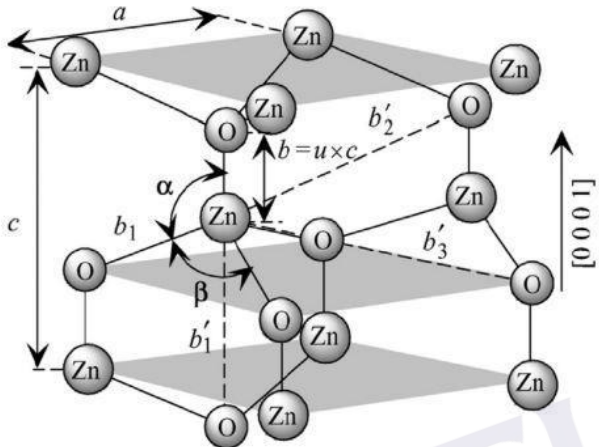


Figure 1.2: Schematic representation of ZnO wurtzite structure [3].

Besides that, ZnO can be synthesized by low-cost production, easy to produce, and allows a good perspective in large scale assembly for the fabrication of thermoelectric modules. There have been numerous reports regarding the fabrication method of ZnO nanostructures either using physical or chemical methods [14]. In this study, ZnO nanostructures will be synthesized by using hydrothermal method. Hence, more details of hydrothermal method will be explained on the next subchapter 2.3.

1.2 Problem statement

The existing zinc oxide nanorods (ZnO-NRs) fabricated using hydrothermal method growth at random orientation on foreign surface that produce non uniform diameter of nanostructures [14]–[17]. These are due to the pure nutrient solution for the hydrothermal method consisting of zinc nitrate hexahydrate (ZNH) and hexamethylenetetramine (HMTA). This process does not include any additive that acts as the catalyst to enhance the growth of ZnO-NRs during the heating process. In the meantime, Y. F. Hsu et al. discovered that using the same material as the seed layer is vital to promote the growth, structure, and orientation of deposited crystals [18]. As ZnO has higher electron mobility ($200\text{--}300 \text{ cm}^2\text{V}^{-1}\text{s}^{-1}$) [19]–[22], alignment is essential to promotes higher electron movement. Hence, seed layer is introduced to initiates the growth of well aligned ZnO nanorods. Furthermore, high resistivity material will resist

REFERENCES

- [1] S. Liu, G. Li, L. Xiao, B. Jia, Y. Gao, and Q. Wang, “Effect of morphology evolution on the thermoelectric properties of oxidized ZnO thin films,” *Appl. Surf. Sci.*, vol. 436, pp. 354–361, 2018.
- [2] J. Kaupužs, A. Medvids, P. Onufrijevs, and H. Mimura, “Origin of n-type conductivity in ZnO crystal and formation of Zn and ZnO nanoparticles by laser radiation,” *Opt. Laser Technol.*, vol. 111, no. March 2018, pp. 121–128, 2019.
- [3] Ü. Özgür, Ya. I. Alivov, C. Liu, A. Teke, M. A. Reschchikov, S. Dogan, V. Avrutin, J. Cho, and H. Morkoc, “A comprehensive review of ZnO materials and devices,” *J. Appl. Phys.*, vol. 98, no. 4, pp. 1–103, 2005.
- [4] X. Zhou, H. Zhang, Q. Chen, J. Shang, and P. Zhang, “Effect of annealing atmosphere on thermoelectric signals from Zno films,” *Thin Solid Films*, vol. 519, pp. 3026–3028, 2011.
- [5] S. Al-lami and H. Jaber, “Controlling ZnO nanostructures morphology on seedless substrate by tuning process parameters and additives,” *Chem. Mater. Res.*, vol. 6, no. 4, 2014.
- [6] A. El-Shaer, A. A. R, and M. M, “Potentiostatic deposition of ZnO nanowires: effect of applied potential and ZnCl₂ concentration,” *Int. J. Res. Eng. Sci.*, vol. 3, 2015.
- [7] Y. Lv, Z. Zhang, J. Yan, W. Zhao, C. Zhai, and J. Liu, “Growth mechanism and photoluminescence property of hydrothermal oriented ZnO nanostructures evolving from nanorods to nanoplates,” *J. Alloys Compd.*, vol. 718, pp. 161–169, 2017.

- [8] B. J. Lokhande and M. D. Uplane, “Structural , optical and electrical studies on spray deposited highly oriented ZnO films,” *Appl. Surf. Sci.*, vol. 167, pp. 243–246, 2000.
- [9] I. Gonzalez-valls, Y. Yu, B. Ballesteros, J. Oro, and M. Lira-cantu, “Synthesis conditions , light intensity and temperature effect on the performance of ZnO nanorods-based dye sensitized solar cells,” *J. Power Sources*, vol. 196, pp. 6609–6621, 2011.
- [10] Z. Zheng, J. Lin, X. Song, and Z. Lin, “Optical properties of ZnO nanorod films prepared by CBD method,” *Chem. Physic Lett.*, vol. 712, no. July, pp. 155–159, 2018.
- [11] O. Marin, V. González, M. Tirado, and D. Comedi, “Effects of methanol on morphology and photoluminescence in solvothermal grown ZnO powders and ZnO on Si,” *Mater. lett.*, vol. 251, pp. 41–44, 2019.
- [12] T. Arakawa and G. Shimaoka, “The epitaxial growth of ZnO thin films on cubic substrates,” *Appl. Surf. Sci.*, vol. 34, pp. 501–508, 1988.
- [13] S. D. N. Luu, T. A. Duong, and T. B. Phan, “Effect of dopants and nanostructuring on the thermoelectric properties of ZnO materials,” *Adv. Nat. Sci. Nanosci. Nanotechnol.*, vol. 10, 2019.
- [14] M. Abdelfatah and A. El-shaer, “One step to fabricate vertical submicron ZnO rod arrays by hydrothermal method without seed layer for optoelectronic devices,” *Mater. Lett.*, vol. 210, pp. 366–369, 2018.
- [15] M. Banari, N. Memarian, and A. vomiero, “Effect of the seed layer on the UV photodetection properties of ZnO nanorods,” *Mater. Sci. Eng. B*, vol. 272, no. June, p. 115332, 2021.
- [16] A. Vomiero, I. Concina, E. Comini, C. Soldano, and M. Ferroni, “One-dimensional nanostructured oxides for thermoelectric applications and excitonic solar cells,” *Nano Energy*, vol. 1, pp. 372–390, 2012.
- [17] M. Skompska and K. Zarębska, “Electrodeposition of ZnO nanorod arrays on

- transparent conducting substrates-a review," *Electrochim. Acta*, vol. 127, pp. 467–488, 2014.
- [18] Y. F. Hsu *et al.*, "Undoped p-type ZnO nanorods synthesized by a hydrothermal method," *Adv. Funct. Mater.*, vol. 18, no. 7, pp. 1020–1030, 2008.
- [19] H. M. Cheng, W. H. Chiu, C. H. Lee, S. Y. Tsai, and W. F. Hsieh, "Formation of branched ZnO nanowires from solvothermal method and dye-sensitized solar cells applications," *J. Phys. Chem. C*, vol. 112, no. 42, pp. 16359–16364, 2008.
- [20] E. Pourshaban, H. Abdizadeh, and M. R. Golobostanfar, "ZnO Nanorods Array Synthesized by Chemical Bath Deposition : Effect of Seed Layer Sol Concentration," *Procedia Mater. Sci.*, vol. 11, pp. 352–358, 2015.
- [21] K. Rahimi and A. Yazdani, "Ethanol-sensitive nearly aligned ZnO nanorod thin films covered by graphene quantum dots," *Mater. Lett.*, vol. 228, no. 3, pp. 65–67, 2018.
- [22] C. Zhou *et al.*, "ZnO for solar cell and thermoelectric application," no. January, 2015.
- [23] H. Ghayour, H. R. Rezaie, S. Mirdamadi, and A. A. Nourbakhsh, "The effect of seed layer thickness on alignment and morphology of ZnO nanorods," *Vacuum*, vol. 86, pp. 101–105, 2011.
- [24] J. Zhang, D. Gao, G. Yang, Z. Zhu, J. Zhang, and Z. Shi, "Study on synthesis and optical properties of ZnO hierarchical nanostructures by hydrothermal method," *Int J Mat Mech Eng*, no. 1, pp. 38–43, 2012.
- [25] M. Raula, M. H. Rashid, T. K. Paira, E. Dinda, and T. K. Mandal., "Ascorbate-assisted growth of hierarchical ZnO nanostructures: sphere, spindle, and flower and their catalytic properties," *Langmuir*, vol. 26, pp. 8769–8782, 2010.
- [26] R. Shi, P. Yang, X. Dong, A. Qian Ma, and A. Zhang., "Growth of flower-like ZnO on ZnO nanorod arrays created on zinc substrate through low-temperature hydrothermal synthesis," *Appl. Surf. Sci.*, vol. 264, pp. 162–170, 2013.
- [27] S. Shaziman, A. S. Ismailrosdi, M. H. Mamat, and A. S. Zoolfakar, "Influence of Growth Time and Temperature on the Morphology of ZnO Nanorods via

- Hydrothermal,” *IOP Conf. Ser. Mater. Sci. Eng.*, vol. 99, no. 1, 2015.
- [28] R. S. Kamel and R. S. Sabry, “Effects of the aspect ratio of ZnO nanorods on the performance of piezoelectric nanogenerators,” *J. Sci. Adv. Mater. Devices*, vol. 4, no. 3, pp. 420–424, 2019.
- [29] I. Udom, M. K. Ram, E. K. Stefanakos, A. F. Hepp, and D. Y. Goswami, “One-dimensional ZnO nanostructures : Synthesis, properties and environmental applications,” *Mater. Sci. Semicond. Process.*, vol. 16, pp. 2070–2083, 2013.
- [30] S. S. Shariffudin, M. Salina, S. H. Herman, and M. Rusop, “Effect of film thickness on structural, electrical, and optical properties of Sol-Gel deposited layer-by-layer ZnO nanoparticles,” *Trans. Electr. Electron. Mater.*, vol. 13, no. 2, pp. 102–105, 2012.
- [31] C. Zuo, D. S. Andrew, and G. Mei, “Drop-Casting Method to Screen Ruddlesden-Popper Perovskite Formulations for Use in Solar Cells,” *ACS Appl. Mater. Interfaces*, vol. 13, no. 47, pp. 56217–56225, 2021.
- [32] Y. Yunus, N. A. Mahadzir, M. N. M. Ansari, T. H. T. A. Aziz, A. M. Afdzaluddin, H. Anwar, M. Wang, A. G. Ismail,, “Review of the Common Deposition Methods of Thin-Film Pentacene, Its Derivatives, and Their Performance,” *Polymers (Basel)*., vol. 14, no. 6, 2022.
- [33] S. Riera-Galindo, A. Tamayo, and M. Mas-Torrent, “Role of Polymorphism and Thin-Film Morphology in Organic Semiconductors Processed by Solution Shearing,” *ACS Omega*, vol. 3, no. 2, pp. 2329–2339, 2018.
- [34] S. Rajamanickam, S. M. Mohammad, and Z. Hassan, “Effect of zinc acetate dihydrate concentration on morphology of ZnO seed layer and ZnO nanorods grown by hydrothermal method,” *Colloids Interface Sci. Commun.*, vol. 38, no. August, 2020.
- [35] Y. Wang and W. Zhou, “A review on inorganic nanostructure self-assembly,” *J. Nanosci. Nanotechnol.*, vol. 10, no. 3, pp. 1563–1583, 2010.
- [36] B. S. Yilbas, A. Al-Sharafi, and H. Ali, *Surfaces for Self-Cleaning*. 2019.
- [37] Z. Cui and L. Liao, “Coating and printing processes,” *Solut. Process. Met.*

- Oxide Thin Film. Electron. Appl.*, 2020.
- [38] K. Gautam, I. Singh, P. K. Bhatnagar, and K. R. Peta, “The Effect of Growth Temperature of Seed Layer on the Structural and Optical Properties of ZnO Nanorods,” *Superlattices Microstruct.*, 2016.
 - [39] J. Park, I. Mahmud, H. J. Shin, M. Park, A. Ranjkesh, D. K. Lee, H. Kim, “Effect of surface energy and seed layer annealing temperature on ZnO seed layer formation and ZnO nanowire growth,” *Appl. Surf. Sci.*, 2015.
 - [40] H. Du, F. Yuan, Ā. S. Huang, J. Li, and Y. Zhu, “A New Reaction to ZnO Nanoparticles,” vol. 33, no. 6, pp. 2–3, 2004.
 - [41] V. Schmidt, J. V. Wittemann, S. Senz, and U. Gósele, “Silicon nanowires: A review on aspects of their growth and their electrical properties,” *Adv. Mater.*, vol. 21, no. 25–26, pp. 2681–2702, 2009.
 - [42] S. O’Brien, M. G. Nolan, M. Çopuroglu, J. A. Hamilton, I. Povey, L. Pereira, R. Martins, E. Fortunato, M. Pemble, “Zinc oxide thin films: Characterization and potential applications,” *Thin Solid Films*, vol. 518, no. 16, pp. 4515–4519, 2010.
 - [43] G. Nam and J. Y. Leem, “Fast-response photoconductive ultraviolet light detectors fabricated using high-quality ZnO films obtained by plasma-assisted molecular beam epitaxy,” *Ceram. Int.*, vol. 43, no. 15, pp. 11981–11985, 2017.
 - [44] J. B. Franklin, B. Zou, P. Petrov, D. W. McComb, M. P. Ryan, and M. A. McLachlan, “Optimised pulsed laser deposition of ZnO thin films on transparent conducting substrates,” *J. Mater. Chem.*, vol. 21, no. 22, pp. 8178–8182, 2011.
 - [45] Y. H. Chen, Y. M. Shen, S. C. Wang, and J. L. Huang, “Fabrication of one-dimensional ZnO nanotube and nanowire arrays with an anodic alumina oxide template via electrochemical deposition,” *Thin Solid Films*, vol. 570, no. PB, pp. 303–309, 2014.
 - [46] S. Rezabeigy, M. Behboudnia, and N. Nobari, “Growth of ZnO Nanorods on Glass Substrate by Chemical Bath Deposition,” *Procedia Mater. Sci.*, vol. 11,

- pp. 364–369, 2015.
- [47] M. Sciences and A. Iowa, “Charge carrier effective mass and concentration derived from combination of Seebeck coefficient and ^{125}Te NMR measurements in complex tellurides E.M Levin,” vol. 50, pp. 1–15, 2016.
 - [48] H. P. Suryawanshi, S. G. Bachhav, and D. R. Patil, “Synthesis and characterization of ZnO nanorod array on FTO glass by using hydrothermal method,” *Techno-Societal 2016*, pp. 645–649, 2018.
 - [49] H. J. Tan, Z. Zainal, Z. A. Talib, H. N. Lim, S. Shafie, S. T. Tan, K. B. Tan, N. N. Bahrudin, “Synthesis of high quality hydrothermally grown ZnO nanorods for photoelectrochemical cell electrode,” *Ceram. Int.*, vol. 47, no. 10, pp. 14194–14207, 2021.
 - [50] X. Li, C. Li, T. Kawaharamura, D. Wang, N. Nitta, M. Furuta, H. Furuta, A. Hatta, “Fabrication of Zinc Oxide Nanostructures by Mist Chemical Vapor Deposition,” *Trans. Mater. Res. Soc. Japan*, vol. 39, no. 2, pp. 161–164, 2014.
 - [51] M.-H. Hong, D. Il Shim, H. H. Cho, and H.-H. Park, “Effect of mesopore-induced strain/stress on the thermoelectric properties of mesoporous ZnO thin films,” *Appl. Surf. Sci.*, vol. 446, pp. 160–167, 2018.
 - [52] L. S. Zambom and R. D. Mansano, “P-ZnO Thin Films Deposited by RF-Magnetron Sputtering,” *J. Phys. Conf. Ser.*, vol. 591, no. 1, 2015.
 - [53] A. Rayerfrancis, P. Balaji Bhargav, N. Ahmed, B. Chandra, and S. Dhara, “Effect of pH on the morphology of ZnO nanostructures and its influence on structural and optical properties,” *Phys. B Condens. Matter*, vol. 457, no. 3, pp. 96–102, 2015.
 - [54] K. Anuar, W. Yee, H. Wah, A. Shin, D. C. S. Bien, and I. Abd, “Effect of seed annealing temperature and growth duration on hydrothermal ZnO nanorod structures and their electrical characteristics,” *Appl. Surf. Sci.*, vol. 283, pp. 629–635, 2013.
 - [55] S. Öztürk, N. Klnç, N. Taşaltn, and Z. Z. Öztürk, “Fabrication of ZnO nanowires and nanorods,” *Phys. E Low-Dimensional Syst. Nanostructures*, vol. 44, no. 6,

- pp. 1062–1065, 2012.
- [56] R. C. Pawar, J. S. Shaikh, N. L. Tarwal, M. M. Karanjkar, and P. S. Patil, “Surfactant mediated growth of ZnO nanostructures and their dye sensitized solar cell properties,” *J. Mater. Sci. Mater. Electron.*, vol. 23, no. 2, pp. 349–355, 2012.
 - [57] C. P. Burke-Govey and N. O. V. Plank, “Review of hydrothermal ZnO nanowires: Toward FET applications,” *J. Vac. Sci. Technol. B Microelectron. Nanom. Struct.*, vol. 31, no. 6, 2013.
 - [58] S. Baruah and J. Dutta, “Hydrothermal growth of ZnO nanostructures,” *Sci. Technol. Adv. Mater.*, vol. 10, no. 1, 2009.
 - [59] N. A. S. Maarof, “Fabrication & characterization of titanium dioxide nanorods and nanoflowers on flourine doped tin oxed (FTO) for ethanol gas sensor application,” Universiti Tun Hussein Onn Malaysia, 2019.
 - [60] M. Ahmad, J. Kiely, R. Luxton, M. Jabeen, and M. Khalid, “Facile aqueous growth of 150nm ZnO nanowires for energy harvester Enhanced output voltage using Pt sputtered electrode,” *Sens. Bio-Sensing Res.*, vol. 7, pp. 141–145, 2016.
 - [61] C. Horachit, S. Moonnoi, P. Ruankham, and S. Choopun, “Effects of precursor concentration on hydrothermally grown ZnO nanorods as electron transporting layer in perovskite solar cells,” vol. 17, pp. 1217–1223, 2019.
 - [62] A. Hassanpour, N. Bogdan, J. A. Capobianco, and P. Bianucci, “Hydrothermal selective growth of low aspect ratio isolated ZnO nanorods,” *Mater. Des.*, vol. 119, pp. 464–469, 2017.
 - [63] M. Ahmad, M. A. Iqbal, J. Kiely, R. Luxton, and jabeen, “Enhanced output voltage generation via ZnO nanowires (50nm): Effect of diameter thinning on voltage enhancement,” *J. Phys. Chem. Solids*, vol. 104, pp. 281–285, 2017.
 - [64] D. Mukhamedshina, K. Mit, N. Chuchvaga, and N. Tokmoldin, “Fabrication and study of sol-gel ZnO films for use in Si-based heterojunction photovoltaic devices,” *Mod. Electron. Mater.*, vol. 3, no. November, pp. 158–161, 2017.

- [65] M. N, H. Mia, S. M. Rana, M. F. Pervez, M. R. Rahman, M. K. Hossain, A. A. Mortuza, M. K. Basher, M. Hoq, "Preparation and spectroscopic analysis of zinc oxide nanorod thin films of different thicknesses," vol. 35, no. 3, pp. 501–510, 2017.
- [66] G. Yang, B. Wang, W. Guo, Q. Wang, Y. Liu, C. Miao, Z. Bu, "Hydrothermal growth of low-density ZnO microrod arrays on nonseeded FTO substrates," *Mater. Lett.*, vol. 90, pp. 34–36, 2013.
- [67] N. K. Abd Hamed, "Study on photocatalytic performance of rutie phased TiO₂ micro size rods/flowers film towards methyl orange degradation," Universiti Tun Hussein Onn Malaysia, 2017.
- [68] F. N. Fahrizal, "Fabrication of nanorod TiO₂/Cu₂O heterostructure thin film," Universiti Tun Hussein Onn Malaysia, 2019.
- [69] C. M. Firdaus, M. S. B. S. Rizam, M. Rusop, and S. R. Hidayah, "Characterization of ZnO and ZnO : TiO₂ Thin Films Prepared by Sol-Gel Spray-Spin Coating Technique," vol. 41, no. Iris, pp. 1367–1373, 2012.
- [70] I. Y. Y. Bu, "Optoelectronic properties of ZnO nanowires deposited under different zinc nitrate/hexamine ratio concentrations," *Ceram. Int.*, vol. 40, no. 4, pp. 6345–6350, 2014.
- [71] A. M. Holi, Z. Zainal, Z. A. Talib, H. N. Lim, C. C. Yap, S. K. Chang, A. K. Ayal, "Effect of hydrothermal growth time on ZnO nanorod arrays photoelectrode performance," *Optik (Stuttg.)*, vol. 127, no. 23, pp. 11111–11118, 2016.
- [72] H. Guo, R. Ding, N. Li, K. Hong, L. Liu, and H. Zhang, "Defects controllable ZnO nanowire arrays by a hydrothermal growth method for dye-sensitized solar cells," vol. 105, no. May 2018, pp. 156–161, 2019.
- [73] R. Khan, U. Periyayya, G. Cheol, and I. Lee, "Fabrication of ultra-sensitive piperidine chemical sensor with a direct grown well-aligned ZnO nanorods on FTO substrate as a working electrode," vol. 97, no. February, 2019.
- [74] H. J. Tan, Z. Zainal, Z. A. Talib, H. N. Lim, S. Shafie, and S. T. Tan, "Sol Precursor Concentration Effect on the Synthesis and Characteristics of ZnO

- Nanoparticles Film," *Int. J. Electroact. Mater.*, vol. 8, no. March, pp. 41–49, 2020.
- [75] S. Patala, "Topological analysis of the grain boundary space," Massachusetts Institute of Technology, 2011.
- [76] S. Pokai, P. Limnonthakul, M. Horprathum, P. Eiamchai, V. Pattantsetakul, S. Limwichean, N. Nuntawong, S. Porntheeraphat, C. Chitichotpanya, "Influence of seed layer thickness on well-aligned ZnO nanorods via hydrothermal method," *Mater. Today Proc.*, vol. 4, no. 5, pp. 6336–6341, 2017.
- [77] B. Ikizler and S. M. Peker, "Effect of the seed layer thickness on the stability of ZnO nanorod arrays," *Thin Solid Films*, vol. 558, pp. 149–159, 2014.
- [78] Y. Y. Liu, C. F. Cheng, S. Y. Yang, H. S. Song, G. X. Wei, C. S. Xue, Y. Z. Wang, "Roughness evolution in Ga doped ZnO films deposited by pulsed laser deposition," *Thin Solid Films*, vol. 519, no. 16, pp. 5444–5449, 2011.
- [79] M. W. Zhu, J. H. Xia, R. J. Hong, H. Abu-Samra, H. Huang, T. Staedler, J. Gong, C. Sun, X. Jiang, "Heat-activated structural evolution of sol-gel-derived ZnO thin films," *J. Cryst. Growth*, vol. 310, no. 4, pp. 816–823, 2008.
- [80] G. Amin, M. H. Asif, A. Zainelabdin, S. Zaman, O. Nur, and M. Willander, "Influence of pH, precursor concentration, growth time, and temperature on the morphology of ZnO nanostructures grown by the hydrothermal method," *J. Nanomater.*, vol. 2011, 2011.
- [81] H. Ungula and H. C. Swart, "study on the role of growth time on structural, morphological and optical properties of un-capped and and l-cyst.-capped ZnO nanorods grown o a GZO seeded thin film layer from aqueous solution," *J. Alloys Compd.*, 2020.
- [82] S. Li, S. Zhou, H. Liu, Y. Hang, C. Xia, J. Xu, S. Gu, R. Zhang, "Low-temperature hydrothermal growth of oriented [0001] ZnO film," *Mater. Lett.*, vol. 61, no. 1, pp. 30–33, 2007.
- [83] A. C. Aragones, A. Palacios-Padros, F. Caballero-Briones, and F. Sanz, "Study and improvement of aluminium doped ZnO thin films: Limits and advantages,"

Electrochim. Acta, vol. 109, no. 3, pp. 117–124, 2013.

